ELSEVIER

Atmospheric Research 79 (2006) 30–51

ATMOSPHERIC RESEARCH

www.elsevier.com/locate/atmos

Individual particles and droplets in continentally influenced stratocumulus: A case study over the Sea of Japan

Daizhou Zhang[a,*], Yutaka Ishizaka[b], Deepak Aryal[b,1]

[a]*Faculty of Environmental and Symbiotic Sciences, Prefectural University of Kumamoto, Kumamoto 862-8502, Japan*

[b]*Hydrospheric–Atmospheric Research Center, Nagoya University, Nagoya 464-8601, Japan*

Received 15 October 2004; accepted 18 April 2005

Abstract

Aerosol particles were collected with an aircraft-borne sampler above, within and below a stratocumulus over the Sea of Japan on December 3, 2000, when continental influence was expected. Particles in the range of 0.3–7 μm and cloud droplets in the range of 0.3–10 μm were captured and they were identified individually upon their elemental composition and morphologies from the analyses by using electron microscopes and an energy dispersive X-ray spectrometer. Interstitial particles and droplets coexisted in the cloud and their number ratio was about 3:2 in the detected ranges. Spherical particles that were inferred to be mainly composed of sulfate, nitrate and ammonium occupied more than 95% of the interstitial particles. Similar particles were also majorities in the above- and below-cloud air, where their percents to total particles were 93% and 74%, respectively. Acidic sulfate particles were rarely found in the below-, in- and even above-cloud air. The nuclei of 90% cloud droplets had similar composition and size distribution to the spherical particles in the scope of our analysis. These results suggest that the continentally influenced stratocumulus was characterized by neutralized nuclei and interstitial particles. Sea-salt particles were detected mainly in the below-cloud air. A few droplets with sea-salt nuclei were detected there and in the cloud. Such droplets were usually larger than those with spherical nuclei but their number

* Corresponding author. Tel.: +81 96 383 2929x761; fax: +81 96 384 6765.
E-mail address: zdz@pu-kumamoto.ac.jp (D. Zhang).
[1] Present address: Central Department of Hydrology and Meteorology, Tribhuvan University, Kirtipur, Kathmandu, Nepal.

doi:10.1016/j.atmosres.2005.04.003

fraction to total droplets in the cloud (about 8%) was much smaller than the spherical nuclei to total droplet fraction, indicating that sea-salt particles produced larger droplets but they constituted only a small number fraction of droplets in the cloud.

Keywords: Cloud droplets and particles; Polluted stratocumulus; Single particle analysis; Aircraft observation; The Sea of Japan

1. Introduction

Clouds have a close relationship with atmospheric aerosol particles. Some particles can act as cloud condensation nuclei (CCN) to produce cloud droplets by water vapor uptake. Inversely, cloud can stimulate new particle formation and cloud droplets can release particles through liquid water evaporation (Twomey and Warner, 1967; Charlson et al., 1987; Hegg et al., 1990; Perry and Hobbs, 1994; Clarke et al., 1998). Besides, phase transformations and chemical reactions including gaseous species, interstitial aerosol particles and liquid droplets are always simultaneously occurring and mutually connected with each other in cloud (Hegg and Hobbs, 1986; Fuzzi et al., 1994; Laj et al., 1997a). These spatial and temporal complexities and the multiphase properties make clouds so complicated that it is difficult to obtain data representing accurate characteristics of aerosol particles and cloud droplets.

Many observations have been conducted to investigate the relationship between cloud droplets and aerosol particles. Comparisons of cloud droplets and interstitial particles revealed that water-soluble particles favor droplet formation more than insoluble particles (Martinsson et al., 1992; Noone et al., 1992; Hallberg et al., 1994; Gieray et al., 1997), and larger particles with larger portions of soluble components were more capable of serving as CCN (Svenningsson et al., 1997). From measurements of residues left by cloud droplet evaporation, Noone et al. (1992), Laj et al. (1997b), and Gurciullo et al. (1999) found that aqueous chemistry in cloud droplets sometimes could lead to changes of particle size and/or composition. If influenced by continental emissions, the processes of cloud droplet formation and depletion would be considerably modified compared to those in an unpolluted atmosphere (Noonkester, 1984; Stephens and Platt, 1987; Hoppel et al., 1990; Garrett and Hobbs, 1995; Bower et al., 2000; Brenguier et al., 2000). For example, it has been reported that the concentrations of Aitken nuclei and CCN in polluted air were much higher than those in clean marine air (e.g., Hudson and Xie, 1999).

The Asian continent is recently characterized by emissions of anthropogenic pollutants (Kato and Akimoto, 1992; Akimoto and Narita, 1994; Galloway et al., 1996; Streets et al., 2003). Due to strong westerlies in winter and spring, pollutants from the continent are usually dispersed eastward to downwind areas. It has been evident that the input of continental pollutants into the downwind marine atmosphere can cause significant changes in the chemistry associated with sulfur dioxide, nitrogen oxides and even chloride (Savoie and Prospero, 1989; Prospero and Savoie, 1989; Parungo et al., 1994; Thornton et al., 1999; Andreae et al., 2000; Zhang and Iwasaka, 2001). However, few in situ observational data on clouds whose gaseous and particulate precursors were influenced by the input are available.

The Sea of Japan is in the downwind area of the Asian continent and the Korean peninsula. Low-pressure systems moving out at altitude from the continent usually stimulate cloud formation in the marine atmosphere (Ishizaka et al., 1995), which provides opportunities to study the influence of continental emissions on clouds in the marine atmosphere.

In this study, we analyzed particles and droplets collected in and out of a stratocumulus during an aircraft observation over the Sea of Japan when continental influence was expected. Morphologies and elemental compositions of individual particles and droplets were obtained using electron microscopes. Compared with measurements by bulk samples that can provide only average information of total collected particulate matters, the single particle analysis can identify the physical and chemical properties of aerosol particles at individual levels and provide more detailed information on particle size and composition, which will consequently help to precisely categorize the particles, study their history and look insight the mutual links between different particles in the atmosphere.

2. Particle collection and analysis

Observations with an aircraft (a King Air B200) were made between 500 m (below cloud) and 3000 m (above cloud) around (35°45′N, 132°36′E) over the Sea of Japan on December 3, 2000. Particles and droplets were collected during 0630–0745 UTC (Local Time=UTC+9 h) when the aircraft flew above, below and in cloud. An in-cloud sample was obtained when the aircraft was descending from 2392 m to 1566 m in cloud, thus it included particles collected at a range of heights. Two above-cloud samples and two below-cloud samples were obtained when the aircraft was turning at same altitudes in above- and below-cloud air, respectively.

Air was introduced into an in-cabin manifold through an inlet. Fig. 1 shows the diagram of the air introduction system. The inlet was fixed below the aircraft cabin facing forward

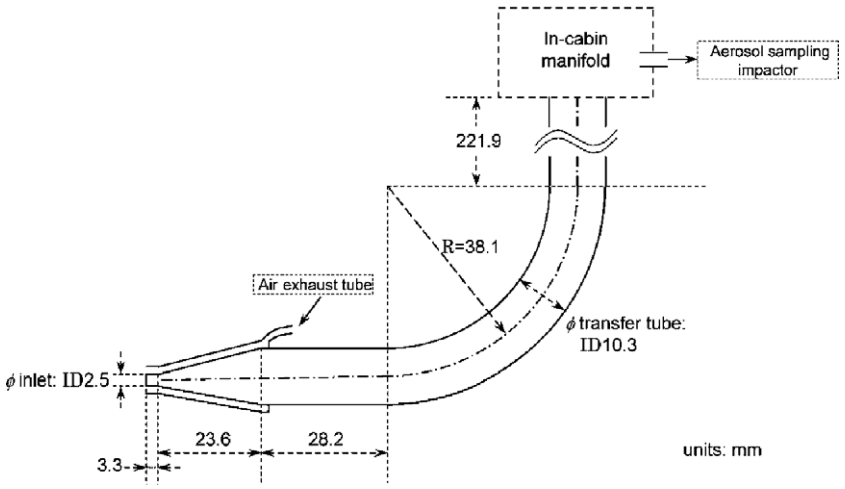

Fig. 1. Schematic diagram of the inlet (not to scale) used to lead ambient air into the in-cabin manifold.

to the flight direction and aligned parallel to the aircraft axis. To avoid flow turbulence at the inlet and minimize the effect of particle collisions on the nozzle edge, a supplementary air exhaust system was made around the inlet and the flow speed into this system was adjusted to keep isokinetic flow at the nozzle. This assured that flow got into the inlet without experiencing turbulence at the inlet entrance, and consequently, the possibility of collisions of particles and droplets was minimized. The manifold was placed directly above the inlet. Introduced air was distributed to a particle collection impactor through a straight tube. The inlet and the manifold were made of stainless steel, which should minimize the influence of electrical charges on the smoothed wall. The pressure inside the aircraft cabin was maintained to be the same as the ambient air. The flight speed during the sampling period was from 70 m s^{-1} to 85 m s^{-1} with an average of 77 m s^{-1}. So the air flow entered the inlet tip at about 77 m s^{-1}; subsequently the conic diffusing section of the inlet decelerated the axial velocity to 4.5 m s^{-1}.

The loss efficiency of particles in the bent section of the inlet was evaluated following Pui et al. (1987) and Blomquist et al. (2001). The curvature ratio of the bent section, which is the ratio of the bend radius (R_{bend}) to the radius of the tube cross-section (R_{tube}), is 7.4. This is within the range of $5 < R_{bend}/R_{tube} < 30$ where the curvature effect has been proven to be insignificant. At 25 °C, pure H_2SO_4 has a density of 1.825 g cm^{-3}, pure HNO_3 has a density of 1.504 g cm^{-3}, pure $(NH_4)_2SO_4$ has a dry particle density of 1.76 g cm^{-3} and pure NaCl has a dry density of 2.17 g cm^{-3}. Hydrated particles with these components will possess densities that are a mixture of these values together with water of hydration at 1.0 g m^{-3}. Transmission efficiencies were calculated for particles with densities of 1.0 and 2.0 g cm^{-3} at a flow rate of 4.5 m s^{-1}. Table 1 shows the diameters at which particles with 1.0 and 2.0 g cm^{-3} densities are transmitted at 90%, 50%, and 10% efficiencies. Theoretically, a particle diameter transmitted with 50% efficiency at 1.0 g cm^{-3} density is 10.8 μm and at 2.0 g cm^{-3} density is 7.6 μm. A particle diameter transmitted with 90% efficiency at 1.0 g cm^{-3} density is 4.2 μm and at 2.0 g cm^{-3} density is 3.0 μm. Because the Reynolds numbers of 5000 inside the conic diffuser and 3000 inside the straight tube were relatively small, turbulence was unlikely to significantly occur inside the diffuser and the tube. Calculations following Muyshondt et al. (1996) were applied to evaluate particle loss caused by the turbulence. The transmission efficiencies of the straight entrance, conic diffuser and straight tube to the manifold (Fig. 1) were calculated separately and then multiplied to deduce the overall transmission efficiency of the entire straight sections. For simplification, the efficiency of the diffuser section was calculated as a cylinder with a diameter of the mean of the tip and tube diameters. Calculated transmission efficiencies for different-size particles with 1.0 or 2.0 g cm^{-3} densities are listed in Table 2. According to these results, loss of particles smaller than 10 μm in the straight sections should be very

Table 1
Estimated transmission efficiencies for the bent section of the inlet (at 20 °C, 1013 hPa)

Particle density (g cm^{-3})	Particle diameter transmitted with various efficiencies (μm)		
	90%	50%	10%
1.0	4.2	10.8	19.7
2.0	3.0	7.6	13.9

Table 2
Estimated transmission efficiencies for the straight section of the inlet (at 20 °C, 1013 hPa)

Particle diameter (μm)	Transmission efficiency with different densities (%)	
	1.0 g cm^{-3}	2.0 g cm^{-3}
5.0	95	94
7.0	94	90
9.0	93	83

small. Particle residence time for the entire inlet length was about 0.07 s. Even a particle with 10 μm diameter and 2.0 g cm^{-3} density, which has its terminal settling velocity of 0.6 cm s^{-1}, would fall only 0.4 mm inside the inlet. Hence the gravitational sedimentation in the inlet was not significant. Overall major particle loss should be caused by the bend in the present inlet system. Aqueous particles and cloud droplets smaller than 10 μm and sea-salt particles smaller than 7 μm can efficiently penetrate the inlet system. Since sea-salt particles were usually smaller than 7 μm, loss of the particles in number was not expected to be significant.

Particles were collected onto electron microscope copper meshes (Maxtaform H7) by using a PIXE Low-pressure Impactor (manufactured by PIXE International Corporation) from the manifold in the aircraft cabin. Only one stage of the impactor (L1) was applied for particle collection and the flow rate was about 3 l min^{-1}. The estimated 50% cutoff diameter of the impactor at 700 hPa is about 0.2 μm and the collection efficiency for particles of 0.3 μm was about 80%. The sampling time for every mesh was 3 min. Sampling meshes were coated with polyvinyl formvar [$(–C_5H_8O_2–)_n$] film sprayed with carbon. After particle collection, each mesh was kept in a plastic capsule. Then the capsule was sealed in a plastic bag together with paper-packaged silica gel, and brought back to the laboratory for subsequent analysis. Samples were investigated using the Hitachi H-9 transmission electron microscope (TEM) of the Hydrospheric–Atmospheric Research Center of Nagoya University. In addition to particle size estimation from the TEM images on mesh film, some particles were identified by their morphologies. According to Frank and Lodge (1967) and Bigg et al. (1970), fresh sea-salt particles are electron-dense (strong absorbability of electrons) squares. If they are aged, their shapes are irregular electron-dense patches. Acidic sulfate particles including sulfuric acid and partially neutralized sulfate particles have distinctive satellite structures: a central spherical spot surrounded by one or more rings of small round spots. Completely neutralized particles are round spots of spherical caps. Particles containing un-dissolved matters are electron-dense spots. These images are created by the collisions or splashes of particles against the film during impaction and the subsequent coagulation after being captured.

Heating tests with electron beams were performed on some particles during TEM analysis. After a picture was taken with weak electron beams, particles in the picture were bombarded with strong electron beams for 5 s. Then the particles were photographed again. Since the samples were kept in capsules which were sealed in plastic bags together with desiccant and the analysis was carried out in high vacuum conditions (10^{-3} to 10^{-4} Pa) in the electron microscope, the particles must have been dehydrated and those in pictures before the bombardment are the residues after dehydration. Consequently, the

residual particles before the heating should be composed of non-volatile and low-volatile components. Here, "low-volatile" means that the compounds do not evaporate or dissociate at room temperature even at 10^{-4} Pa within a few minutes. With the increased strength of electron beams hitting particles, the particles were heated and the low-volatile compounds would evaporate and escape from the particles causing the particles to change in morphology. By this test, we determine whether the particles contained low-volatile compounds.

Particles and droplets, including many on TEM pictures, were also investigated using the SEMEDX system (a Hitachi S-3000N scanning electron microscope equipped with a Horiba EMAX-500 energy dispersive X-ray spectrometer) of the Solar Terrestrial Environment Laboratory of Nagoya University. With this SEMEDX, we measured relative weight and atom ratios of elements of atom number (Z) larger than 5 except nitrogen in a single particle or droplet down to 0.1 μm. In this study, we applied the data of elemental compositions of particles and droplets to confirm their categorization.

3. Weather, observed cloud and backward trajectories

Fig. 2 shows the GMS Visible Image at 0600 UTC, surface weather chart at 0000 UTC on December 3, 2000, and the isentropic backward trajectories of the below-, in- and above-cloud air masses. The aircraft observations were carried out about 3 h after a cold front had passed through at the surface. A strong northwesterly flow in elevated layers was noted during the sampling period. Cloud images recorded by an on-board CCD camera and the cloud information later published by Japan Meteorological Agency indicated that the cloud we measured was a stratocumulus with its base at 1000 m and top at 2500 m, which was of typical cloud behind low-pressure centers in this area in winter (Ishizaka et al., 1995).

The isentropic backward trajectories indicate that the below- and in-cloud air masses were from low levels near the ground in eastern China and they moved upward in the troposphere as they slowly moved northeastward there. The above-cloud air masses moved upward over western China where anthropogenic activities are much less than in eastern China. Therefore, air masses around the cloud, particularly those in and below the cloud, should have been significantly influenced by anthropogenic emissions from China and Korea. It is also learnt from the trajectories that the air masses left the Asian continent, crossed over the Korean peninsula and arrived at the sampling area within about 1 day, suggesting the air masses retained the characteristics of land emission influence.

The thermodynamic structures of vertical layers, which were obtained by a Rawinsonde launched at Yonago (35°30′N, 133°54′E) near the observational area at 1200 UTC on December 3, 2000, are shown in Fig. 3. The potential temperature profile indicates the layer from surface to the cloud base has been well mixed but there was a thin inversion layer at the cloud base (about 1800 m) which separated the cloud layer from the lower below-cloud air masses. In cloud, the vertical distributions of relative humidity and equivalent potential temperature are not consistent with the moist adiabatic lapse rate, suggesting the in-cloud updraft was weak. At cloud top, there was an inversion and strong hydrolapse, suggesting that the vertical mixing above the cloud top should be extremely

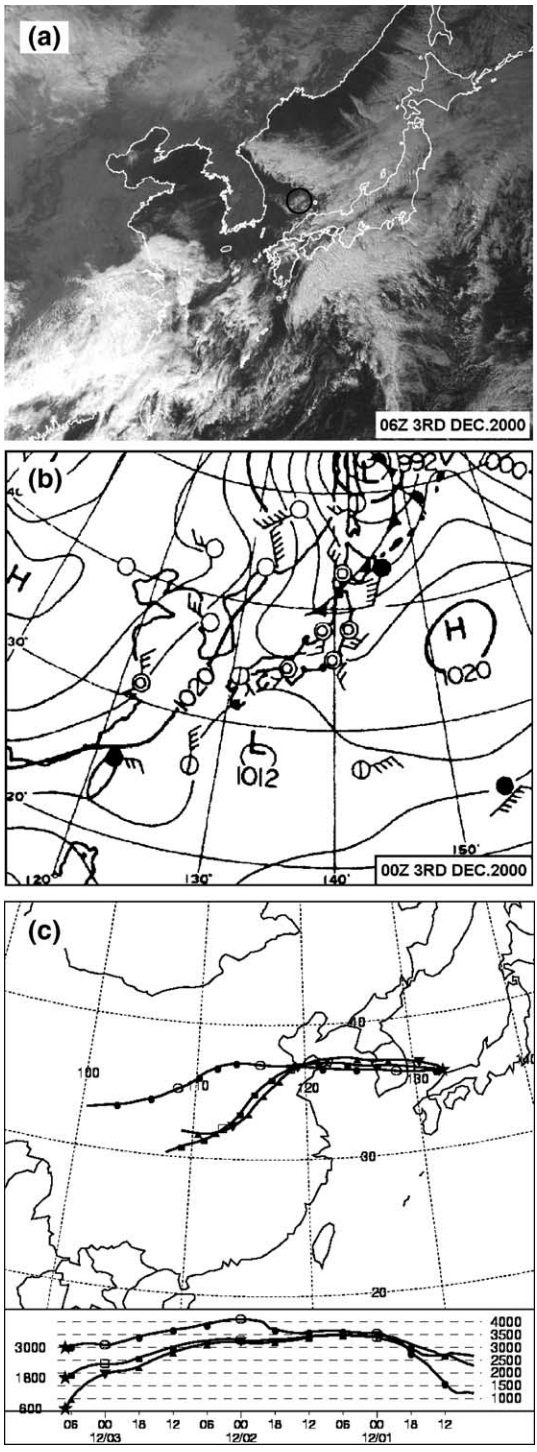
(a)
06Z 3RD DEC.2000
(b)
H
1020
1012
30°
20°
120°
130°
140°
150°
00Z 3RD DEC.2000
(c)
100
10
20
30
40
80
3000
1800
600
4000
3500
3000
2500
2000
1500
1000
06 00 18 12 06 00 18 12 06 00 18 12
12/03
12/02
12/01

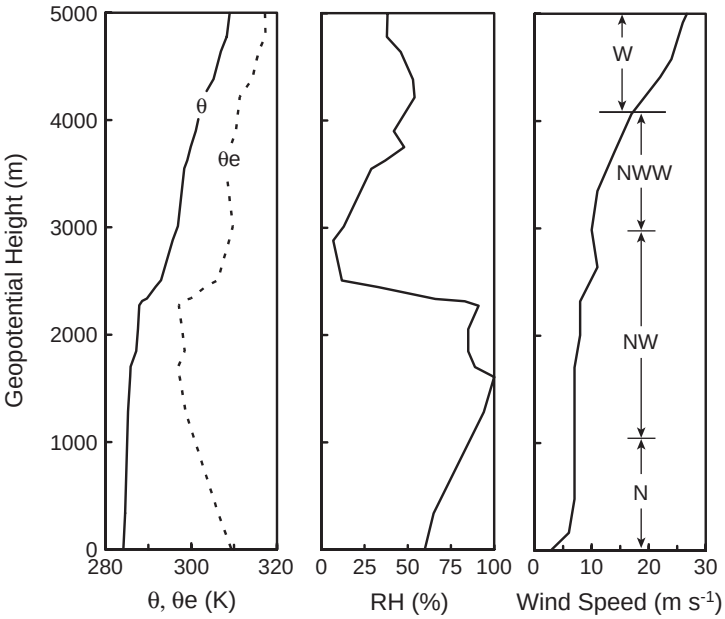

Fig. 3. Vertical profiles of potential temperature θ, equivalent potential temperature θe, relative humidity RH, and wind speed and direction at Yonago (35°30′N, 133°54′E) at 1200 UTC, December 3, 2000.

weak. Below 500 m, wind speed had strong vertical shear from 3 m s^{-1} at 8 m to 7 m s^{-1} at 480 m, further suggesting strong vertical mixing in the surface layer.

4. Results

4.1. Morphology

Fig. 4 shows the typical pictures of samples in the below-, in- and above-cloud air. The majority of below-cloud particles are round spots (such as particle A in Fig. 4a) and irregular electron-dense particles (particle B in Fig. 4a). The round shape of spots on the film indicates that they were in the aqueous phase before being captured and that these particles should be spherical in the air, i.e., they were wet aerosol particles. Hereafter, such particles are denoted as "spherical particles" and irregular electron-dense particles are denoted as "irregular particles." The spherical particles were usually smaller than the irregular particles. Besides the spherical and irregular particles, there were some other

Fig. 2. (a) Satellite image (VIS) at 0600 UTC. The circle on the image marks the observation area. (b) Surface weather chart at 0000 UTC on December 3, 2000. (c) 72-h isentropic backward trajectories of below-cloud (600 m), in-cloud (1800 m) and above-cloud (3000 m) air masses over the observation site (35°45′N, 132°36′E) from 0700 UTC on December 3, 2000. The trajectories were calculated by the HYSPLIT model of NOAA Air Resources Laboratory's web server (/www.arl.noaa.gov/).

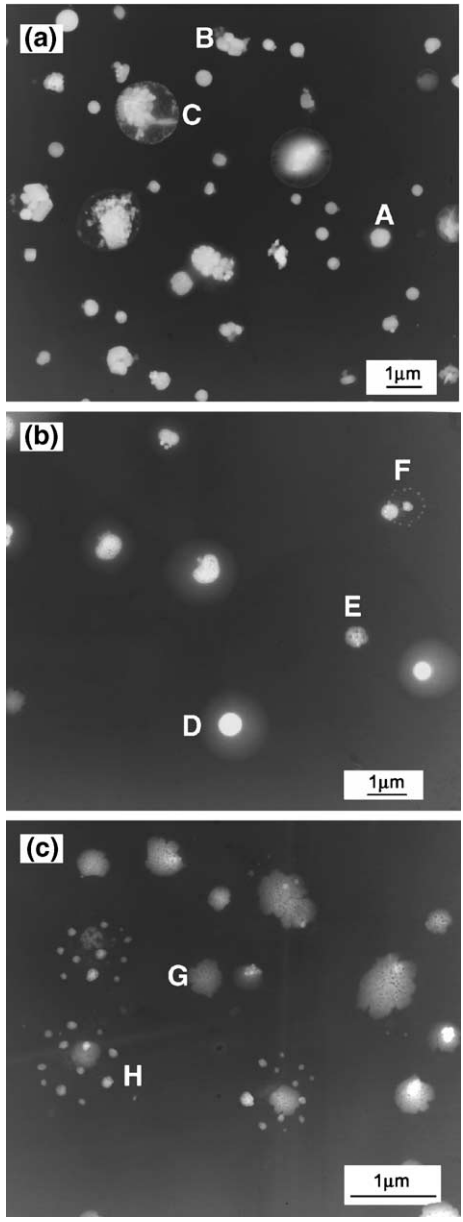

Fig. 4. TEM pictures of particles collected (a) below, (b) in, and (c) above the cloud. The pictures, also in Fig. 5, are black–white reversed ones. Electron-dense parts of particles are bright in white.

particles which had irregular electron-dense cores with outside circles (particle C in Fig. 4a). They are apparently different from the spherical and irregular particles. The round shape of the circles indicates that the particles had an aqueous surface layer before being

captured. That suggests that the particles were droplets or deliquesced haze particles in below-cloud air and that the central irregular electron-dense cores were their condensation nuclei acquiring water vapor. Since the areas of central irregular cores in most of such particles were apparently smaller than the areas between the cores and their outside circles, they were more likely droplets. Hereafter, these nuclei are denoted as "irregular nuclei" and the droplets are denoted as "droplets with irregular nuclei".

In the cloud, a lot of particles showed the morphology of a round spot surrounded by a ring (D in Fig. 4b). There were not apparent electron-dense materials in the surrounding ring areas while the central spots had similar morphology to that of below-cloud spherical particles. Considering their distinguishable morphology and the fact that similar particles were rarely found out of the cloud, these particles are believed to be cloud droplets. There were also a large number of round spots in the cloud (particle E in Fig. 4b) and they had similar morphology to the below-cloud spherical particles, indicating the presence of spherical particles in the interstitial air. A few particles with satellite structure appeared in the interstitial air (particle F in Fig. 4b), indicating the presence of acidic sulfate particles.

Above the cloud, the majority of particles were those similar to spherical particles in the below- and in-cloud air (particle G in Fig. 4c). Besides, there were some acidic sulfate particles (particle H in Fig. 4c). Few other particles were detected there.

4.2. Volatility and elemental composition

Fig. 5 shows changes of particles and droplets before and after the electron heating. Below-cloud spherical particles had apparent changes (particle I in Fig. 5a and b), indicating some components evaporated and escaped while the irregular particles had no apparent changes (particle J in Fig. 5a and b). Interstitial spherical particles in cloud changed similarly to the below-cloud spherical particles but the cloud droplets were different (Fig. 5c and d). The surrounding rings of droplets did not change but their central spots changed similarly to the below-cloud and interstitial spherical particles. The above-cloud spherical particles also changed similarly to the below-cloud and interstitial spherical particles (figures are not shown). Therefore, the spherical particles in the below-, in- and above-cloud air, and the round spots of cloud droplets had similar volatility characteristics.

Only sulfur among elements with $Z>10$ was detected from spherical particles like particles A, E, and G. Even after electron heating, such particles had similar spectra. An example of the X-ray spectra is shown in Fig. 6a. The elemental compositions of irregular particles such as particle B and the irregular nuclei of below-cloud droplets such as particle C are very different from the spherical particles. They were mainly composed of sodium and chlorine with minor magnesium and sulfur (Fig. 6b), suggesting they were sea-salt particles or modified sea-salt. Since the compositions of all irregular particles and irregular droplet nuclei in the extent of our analysis were similar to that shown in Fig. 6b, we think all irregular particles are sea-salt particles and all droplets with irregular nuclei in this study are droplets with sea-salt nuclei.

The ring areas of cloud droplets as in particle D did not generate detectable X-rays except those caused by meshes (Cu) and films (C and O). However, the central spots of droplets contained only sulfur among the elements with $Z>10$ both before and after

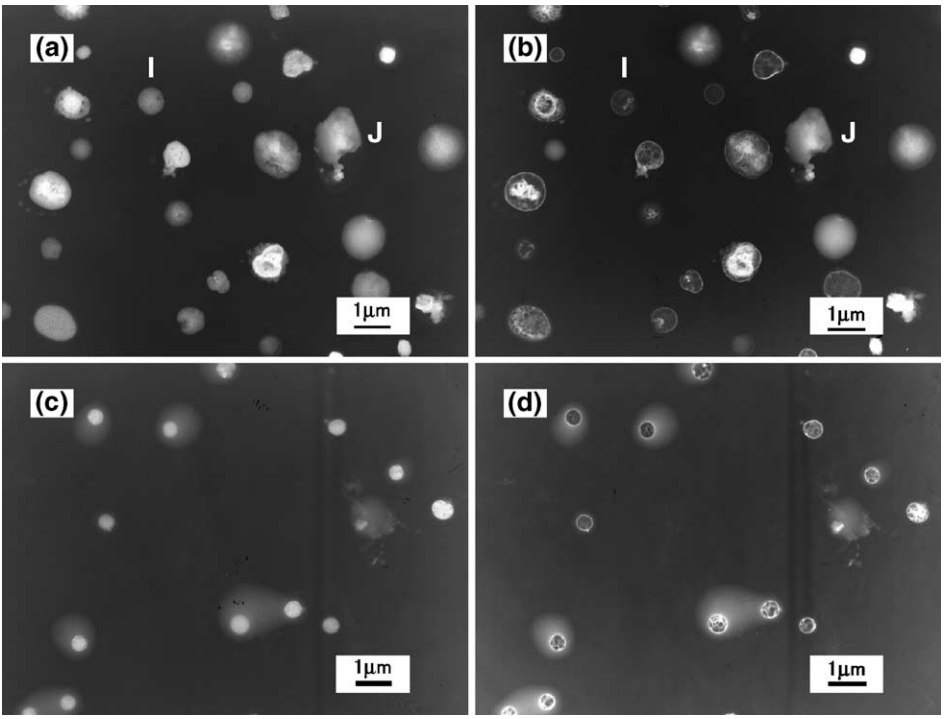

Fig. 5. TEM pictures of below-cloud particles [(a), (b)] and in-cloud particles [(c), (d)] before and after electron heating, respectively.

heating, further suggesting that their composition is similar to the spherical particles in and out of the cloud. A plausible interpretation for the morphology of the droplets is that the rings are vestiges left by liquid water evaporation and the central spots are coagulated water-soluble substances in the droplets. As discussed in the following sections, it is believed that the central spots retained major characteristics of the CCN on which the droplets were formed initially. Hereafter for distinguishing from irregular nuclei, the central round spots are denoted as "spherical nuclei," and the droplets formed on the spherical nuclei are denoted as "droplets with spherical nuclei".

4.3. Number fractions

In order to evaluate the contribution of different particles and droplets in and out of the cloud, their number fractions in particles and droplets were estimated. Particles and droplets were identified by their morphologies on TEM pictures as shown in Fig. 3. Pictures applied for the estimation covered the mesh holes along a diameter across the impaction center on the mesh. The results are listed in Table 3. It should be noted that only particles/droplets larger than 0.3 μm could be efficiently captured by the impactor, and cloud droplets larger than 10 μm and sea-salt particles larger than 7 μm, if they existed, were cut by the inlet. Since the majority of accumulation mode aerosol particles

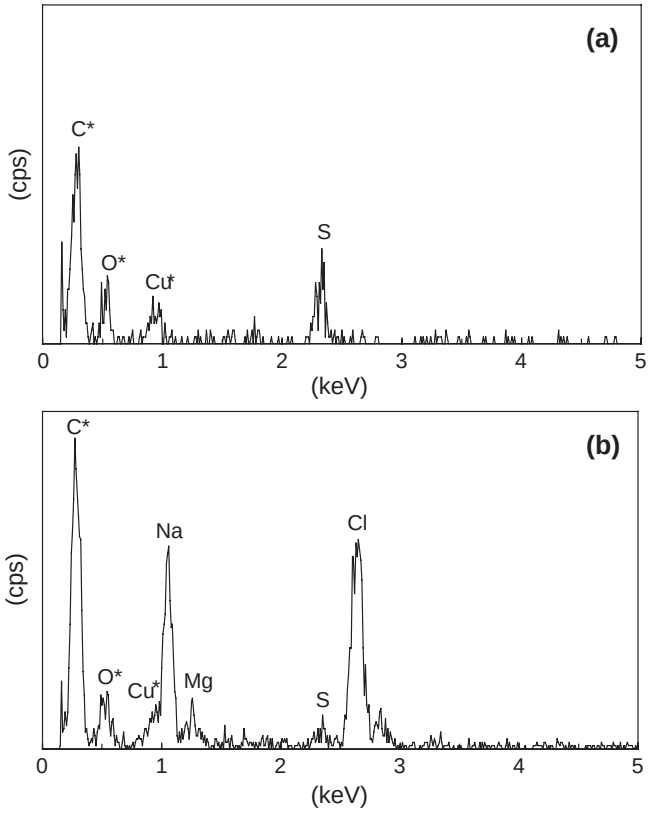

Fig. 6. X-ray spectra for spherical particles (a) and irregular particles (b). Elements marked with asterisk ("*") in the spectra were caused or distorted by the sampling meshes and the carbon pedestal for SEMEDX analysis.

should be around 0.3 μm or smaller, most of them must have been lost. In the cloud, interstitial spherical particles and cloud droplets together occupied more than 97% in number and the ratio of interstitial particles to droplets was about 3:2 in the detected ranges. Spherical particles were also the majority in the interstitial air and they occupied about 95% of interstitial particles. Further investigation of cloud droplet nuclei revealed

Table 3
Number fractions (%) of different particles in and out cloud

Particle category	Below cloud	In cloud	Above cloud
Spherical particles	74	58	92
Droplets	3	39	N.D.[a]
Irregular particles	22	2	2
Acidic sulfate particles	≪1	1	5
Others	1	N.D.[a]	≪1
Total detected particles	1362	877	1060

[a] N.D.—not detected.

that 90% of them were spherical nuclei, and droplets with sea-salt nuclei accounted for 8% of in-cloud droplets (Table 4), which is consistent with the results of Hudson and Da (1996).

In the above- and below-cloud air, the majority of particles were the spherical ones and their number fractions were 92% and 74%, respectively. Sea-salt particles were mainly in the below-cloud air and they occupied 22% there. A few droplets were detected in the below-cloud air and most of them were droplets with sea-salt nuclei. No droplets were detected in the above-cloud air. In addition, acidic sulfate particles were rarely found in the below- and in-cloud air. A few were detected in the above-cloud air and their number fraction was 5% there.

4.4. Size distributions

Particles and droplets were sized by their morphologies on TEM pictures. Here we applied the diameters of particle and droplet images on mesh films as their sizes, hereafter denoted as on-film diameters. In single particle analysis, the geometric diameter of a particle before being captured is usually estimated from its on-film image with the assumption that the particle is spherical in the atmosphere and has the same volume to its on-film one (Ayer, 1978). We do not use such estimation here since it has large uncertainties and is invalid for droplets. Our purpose is to compare the size ranges of particles and droplets. On-film diameters as defined hereafter can meet this purpose. The on-film diameter of a spherical particle or a spherical nucleus of a droplet was designated as the diameter of its image on the collection film, that of an irregular particle or an irregular nucleus as the average of its length and width, and that of a droplet as the diameter of the outside circle of its ring. Assuming that spherical particles and droplets on the film after impaction are hemi-spherical with their volume the same as the volume before being captured, their on-film diameters should be about 1.3 times their geometric diameters. Because aqueous particles can hardly maintain their hemi-sphere shape on a flat film, and because the larger the particles the easier their expansion, the on-film diameters of spherical particles and droplets with spherical nuclei should be 1.3 times their geometric diameter or larger. According to McInnes et al. (1997), on-film diameters of sea-salt particles are approximately the same as their aerodynamic ones. Consequently in the case of a droplet with sea-salt nucleus, the geometric diameter of the droplet should be an intermediate of its on-film diameter and its irregular nucleus on-film diameter.

The distributions of particles, droplets and droplet central nuclei are illustrated in Fig. 7. They are not usual number–size distributions but tentative ones of counted particles and

Table 4
Number fractions (%) of different nuclei of droplets below and in cloud

Nuclei category	Below cloud	In cloud
Spherical nuclei	8	90
Irregular nuclei	90	8
Others	2	2
Total detected droplets	39	340

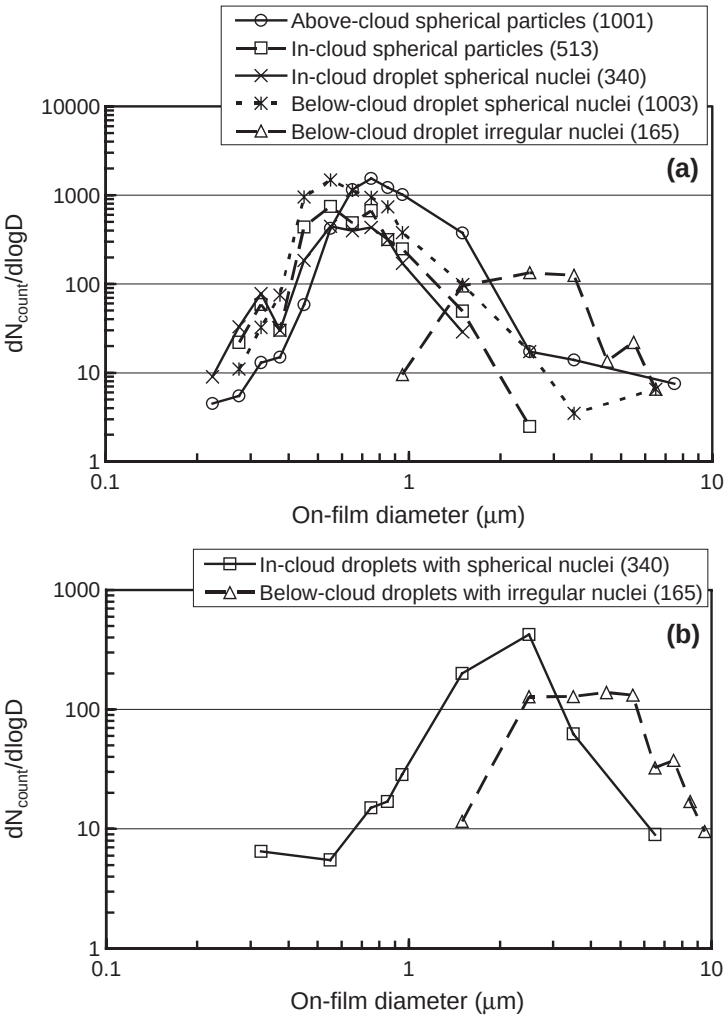

Fig. 7. (a) Number–size distributions of spherical particles at different places regarding to the cloud and those of droplet nuclei, and (b) number–size distributions of droplets with spherical nuclei in cloud and droplets with irregular nuclei below cloud. The distributions of below-cloud droplets and their nuclei were from particles on pictures of selected areas in which an adequate number of droplets were available for statistical estimation. Others were from pictures for the number–fraction estimation. Data in the parentheses are numbers of counted particles and droplets. Diameters are the on-film diameters (see the definition in the text).

droplets to on-film diameter. Spherical particles and droplets with spherical nuclei were mainly in the on-film diameter range of 0.2–6 μm with their peaks at 0.6–0.9 μm and at 1–4 μm, respectively. Sea-salt particles in the below-cloud air had their on-film diameter range of 0.9–7 μm with its peak at 2–3 μm and droplets with sea-salt nuclei had their range of 1–10 μm with its peak at 3–5 μm. Since the sampling system was effective for particles in the range of 0.3–7 μm and for cloud droplets in the range of 0.3–10 μm of aerodynamic

diameters, the results for particles and droplets shown in the figure are reasonable except that particles smaller than 0.5 μm on-film diameters might have been largely underestimated. The distributions of spherical particles inside and outside the cloud and that of spherical nuclei of in-cloud droplets are approximately consistent with each other (Fig. 7a). Although the inlet system might have resulted in the loss of sea-salt particles and droplets with sea-salt nuclei in the range larger than 7 μm in the below-cloud samples, the distribution of sea-salt nuclei was apparent in larger size ranges than spherical particles, and that of droplets with sea-salt nuclei is apparent in larger size ranges than droplets with spherical nuclei (Fig. 7a,b).

5. Discussion

5.1. Mixture of the spherical particles

Spherical particles were predominant inside and outside the cloud. The existence of sulfur in them suggests that they contained sulfate. Since they did not show acidic nature, sulfate in these particles must have been completely or almost completely neutralized in the form of sulfate or bi-sulfate. The neutralizer is probably ammonia. One reason is that ammonia is the unique alkaline gas in the atmosphere and it is constantly emitted from land sources and sea surface (Galloway et al., 1996; Dibb et al., 1999). Another reason is that ammonia does not contain elements with $Z > 10$, which is consistent with the particle elemental composition. Therefore, the spherical particles are believed to contain ammonium and sulfate. The heating test revealed that they contained low-volatile compounds. The most common compounds associated with ammonium in marine atmosphere are ammonium sulfate and ammonium nitrate. Considering that ammonium nitrate is much more volatile than ammonium sulfate and the fact that sulfur was still detected in the particles after heating, the escaped component is more likely ammonium nitrate. In other words, the spherical particles could possibly contain nitrate in addition to sulfate.

Analysis of bulk aerosol samples that were collected onboard simultaneously in the present study by a low volume sampler on nuclepore filters revealed that in the below- and in-cloud air the ratios of the concentration of major cations to that of major anions in the samples were a little larger than 1. Particularly in the sample which was collected when the aircraft descended from cloud into below-cloud air (3 min in cloud and 2 min below cloud), the major anions were nitrate (30.6) and sulfate (21.4) besides chloride (34.8) and the major cation was ammonium (12.5) besides sodium (46.2), magnesium (26.2) and calcium (12.9) (all in neq m^{-3}; from Kagawa et al., 2001), indicating that there was considerable excess ammonia after total sulfate was neutralized. The presence of excess ammonia could have led to nitrate deposition onto the particles (Stelson and Seinfeld, 1982; Matsumoto and Takana, 1996). The presence of ammonium nitrate in aerosol particles around cloud and in cloud droplets was also testified by many observations such as Fuzzi et al. (1994), Watanabe et al. (2001), and Kaneyasu et al. (2001). The extra ammonia is presumably from Asian continent and/or Korean peninsula because ammonia emission in China is very large and its rapid increase in recent decades has been predicted

(Galloway et al., 1996; Streets et al., 2003). Observations in coastal areas of China proved that acidic materials in secondary particles in surface atmosphere could be completely neutralized by ammonia from anthropogenic sources (Zhang et al., 2000).

The concentration of acidic sulfate particles was relatively high and the concentration of sea-salt particles was relatively low in the above-cloud air compared to those in the below- and in-cloud air, indicating the particles below and above-cloud top had different chemical natures. The vertical thermal structure shown in Fig. 3 revealed the stratocumulus was capped by a strong inversion and the upward mixing was very weak at the cloud top. The isentropic backward trajectories indicate that the influence from continental surface emissions on the below- and in-cloud air masses was more significant than that on above-cloud air masses (Fig. 2), which supports the analysis results of particles at different levels.

5.2. Spherical nuclei

It is expected that uptake of gaseous species onto cloud droplets would not change the original CCN considerably. One reason is that the pH of cloud water is usually around 4.0 and the concentration of hydrogen peroxide (H_2O_2) in cloud water is very low over the Sea of Japan in winter (Watanabe et al., 2001). In the present case, bulk cloud water was collected with a cloud water collector when the aircraft was descending in the cloud. The collection efficiency of the collector for droplets with diameter of 10 μm is 30–40% (Suzuki and Horibe, 2001). The collected cloud water was reserved in cooling (<10 °C) and sent to laboratory for analysis right after the aircraft landed. The concentrations of Na^+, NH_4^+, Mg^{2+} and Ca^{2+} in the cloud water were 302.39, 200.40, 106.04 and 68.78 μeq l^{-1}, and that of Cl^-, NO_3^- and non-sea-salt SO_4^{2-} were 201.42, 166.81, and 381.57 μeq l^{-1}, respectively. The pH of the cloud water was 4.1, the ratio of the concentration of total cations to that of total anions was 0.98, and H_2O_2 concentration was 0.37 μM (Kagawa et al., 2001), which should have depressed the aqueous-phase production of sulfate through S(IV) oxidation by H_2O_2 (Martin and Damschen, 1981). Another reason is that the cloud we observed developed over the Sea of Japan and its history was so short that the oxidants such as H_2O_2 were not expected to largely modify the chemical contents of particles and droplets. Otherwise, the modifications through S(IV) conversions in the particles and droplets by oxidants such as O_3 were similar. In that sense, we still think that the spherical nuclei were similar to the spherical interstitial particles. Our analysis has shown that the detectable elements in the nuclei are only sulfur and sizes of spherical nuclei are similar to those of spherical particles. Even if coalescence, coagulation and aqueous phase reactions might have resulted in a little quantitative change of the droplet nuclei, the qualitative changes of the nuclei were not identified. Thus, the spherical nuclei, to a large extent, could represent the major characteristics of the original CCN, suggesting the droplets with spherical nuclei were formed on particles similar to the spherical particles.

There were a large number of spherical particles in the cloud interstitial air. Although their composition and size are similar to the spherical nuclei of most cloud droplets, they existed as interstitial particles rather than in cloud droplets. Possible input of aerosol particles from the below-cloud air could not account for their presence because there was a

thin inversion layer at the cloud base and the number fraction of irregular particles in the interstitial particles in cloud, 0.04 (2/58 from Table 3), was much smaller than that in below-cloud air, 0.3 (22/74 from Table 3). With a mechanism of ripening process, Celik and Marwitz (1999) investigated the roles of the curvature and salinity of CCN in droplet formation. They suggested that the growth of larger droplets that had smaller equilibrium supersaturation would decrease the supersaturation in cloud, and this would lead to the evaporation of small droplets that had larger equilibrium supersaturation even if the ambient relative humidity remained larger than 100% in case of weak updraft. However, this seems not the case in this study because the ratio of interstitial spherical particles to cloud droplets is quite large (Table 3) and the observations were made in a polluted air mass in which all particles were very unlikely to be good CCN. It is hard to believe that such a large fraction of aerosol particles activating once to have produced droplets experienced significant evaporation to return to aerosol particles in a supersaturated or just saturated environment.

It is more likely that the interstitial spherical particles were deactivated particles. In general, when interstitial particles contain large fractions of water-insoluble compounds besides ammonium, sulfate and nitrate, the insoluble components increase the critical supersaturation needed to form cloud droplets (Martinsson et al., 1992; Hallberg et al., 1994; Gieray et al., 1997). Organic compounds may be the source of such insoluble material (Anttila and Kerminen, 2002; Shantz et al., 2003). Our methods are not effective to detect water-soluble organic aerosol components. It is noted that water-insoluble organic components such as black carbons that present as soot are usually small spheres or sphere chains on electron microscope mesh films. Such soot particles are detectable by the techniques in this study (Parungo et al., 1994; Zhang et al., 2001). Bombardment of electrons cannot change their morphologies in electron microscopes as shown in Fig. 5 and carbon in the particles is detectable with the comparisons of X-ray spectrums of background films and that of particles. In the scope of our analysis, we did not find such components either in the interstitial spherical particles or in the spherical nuclei and did not find any significant differences between them. So the reasonable explanation for the existence of substantial spherical particles in the cloud interstitial air is likely that the particles contained water-insoluble organics but no soot-like components appeared with the organics or the masses of the organics were too small to be detected by our methods. The analysis by Kagawa et al. (2001) did find acetate and formate in the cloud water and their concentrations were 23.11 and 4.06 μeq l^{-1}, respectively, indicating the presence of organics in cloud droplets.

5.3. Droplets formed on sea-salt particles

A few droplets as large as 10 μm were found in the below-cloud air. In contrast to the droplets in the cloud, most of the below-cloud droplets were formed on sea-salt particles. Sea-salt particles can form droplets due to their high deliquescence but the question is why the droplets presented in the below-cloud air. One possibility is that the sea-salt particles in the below-cloud air acquired water coating since the ambient relative humidity was nearly 80% (Fig. 3). If this is true, the simultaneous presence of particles of types B and C suggests some sea-salt particles can become wet aerosols or activate to form droplets when

the relative humidity is around 80%. Another possibility is that the droplets were drizzle drops dropping out from the cloud base due to their large sizes.

The droplets with spherical particles had a narrow peak range of 1–4 μm, which was consistent with their neutralized nature since droplets in continentally polluted clouds usually have small mean diameter of droplets (<10 μm) and narrow droplet spectra (e.g., Hudson and Li, 1995). In contrast, droplets formed on sea-salt particles were in larger ranges. This phenomenon is plausible since larger particles form larger droplets and smaller particles smaller droplets by water vapor condensation (Hudson and Rogers, 1986; Noone et al., 1992; Kramer et al., 2000; Schwarzenbock et al., 2001). It should be noticed that this would result in the volume and mass contributions of droplets with sea-salt nuclei much larger than the contributions of droplets with spherical nuclei. Although their number was much less than droplets with spherical nuclei in the cloud (this study), droplets with sea-salt nuclei had made ion concentrations of sodium and chloride larger than sulfate and nitrate in the bulk cloud water (Kagawa et al., 2001: data raised in Section 5.1). The potential significance of this result is that, while sodium and chloride were substantially detected from bulk cloud water, suggesting sea-salt particles acted as cloud droplet nuclei, the fact might be that cloud droplets formed on sea-salt particles were in a minority in marine stratocumulus. It should be noted that the contribution of sea-salt particles to CCN fraction is likely to depend on surface wind speed, as well as factors such as boundary layer depth and the state of boundary layer mixing in the vertical in the marine atmosphere. Even if the numbers of sea-salt CCN are small, they maybe important because of their size for initiating drizzle in stratocumulus cloud.

6. Summary

In this study, the aerosol particles in the range of 0.3–7 μm and droplets in the range of about 0.3–10 μm below, within and above continentally influenced stratocumulus over the Sea of Japan were analyzed using a TEM and a SEMEDX. With the morphologies and elemental compositions of the particles and droplets, their categories, formations, and mutual links both within and outside the stratocumulus were described and discussed.

The stratocumulus was characterized by neutralized interstitial particles and droplets with neutralized nuclei. The number ratio of interstitial particles to cloud droplets was about 3:2 in the detected ranges. Spherical particles that were inferred to be mainly composed of sulfate, nitrate and ammonium occupied more than 95% of the interstitial particles in number. Other particles such as sea-salt particles were rarely detected. The nuclei of about 90% cloud droplets were similar to the spherical particles in the scope of our analysis. Droplets formed on sea-salt particles constituted merely 8% of cloud droplets, suggesting that sea-salt particles might not be important for cloud droplet formation in terms of droplet number, although sea-salt usually constitutes large fractions of ions in bulk cloud water in marine stratocumulus.

Spherical particles were the majorities also in the above- and below-cloud air and they occupied 92% and 74% of particles, respectively. Sea-salt particles were mainly found in

the below-cloud air and they occupied 22% of total particles there. Acidic sulfate particles were rarely found even in the above-cloud air.

This is a try to study droplets and particles in and out continentally influenced stratocumulus by single particle analysis using electron microscopes. Results reported here are from two above-cloud samples, two below-cloud samples and one in-cloud sample during an aircraft mission. The results should closely depend on the stratocumulus and weather conditions. No similar observations and analyses are available for comparisons yet. In addition, water-soluble organics and most of volatile components are not detected because of the limit of our methods. The statistical results in Table 3, Table 4 and Fig. 7 are from tiny numbers of particles compared to other techniques such as optical particle counters. Special attentions should be paid to these points in the comparisons of this study with other observations.

Acknowledgments

The authors express their appreciation to Dr. Y. Iwasaka for his support in the SEMEDX analyses. The authors wish to thank Dr. A. Matsuki and Mr. K. Suzuki for their assistance in the investigation of particle transmission efficiency of the inlet. The authors also hope to show their special thanks to the two anonymous reviewers. Their detailed comments and suggestions helped to increase largely the quality and readership of this paper. This work was carried out under the Research Fund of Special Research Project of the Institute of Hydrospheric–Atmospheric Sciences of Nagoya University. Financial support was also provided partly by the Japan Science and Technology Corporation, the CREST program 1999–2004 (Chief Scientist: Prof. T. Nakajima, CCSR, University of Tokyo).

References

Akimoto, H., Narita, H., 1994. Distribution of SO_2, NO_x and CO_2 emissions from fuel combustion and industrial activities in Asia with $1^\circ \times 1^\circ$ resolution. Atmospheric Environment 28, 213–225.

Andreae, M.O., Elbert, W., Gabriel, R., Johnson, D.W., Osborne, S., Wood, R., 2000. Soluble ion chemistry of the atmospheric aerosol and SO_2 concentrations over the eastern North Atlantic during ACE-2. Tellus 52B, 1066–1087.

Anttila, T., Kerminen, V.M., 2002. Influence of organic compounds on the cloud droplet activation: a model investigation considering the volatility, water solubility, and surface activity of organic matter. Journal of Geophysical Research 107 (D22), 4662. doi:10.1029/2001JD001482.

Ayer, G.P., 1978. Quantitative determination of sulphate in individual aerosol particles. Atmospheric Environment 12, 1613–1621.

Bigg, E.K., Ono, A., Thompson, J.A., 1970. Aerosols at altitudes between 20 and 37 km. Tellus 22, 550–563.

Blomquist, B.W., Huebert, B.J., Howell, S.G., Litchy, M.R., Twohy, C.H., Schanot, A., Baumgardner, D., Lafleur, B., Seebaught, R., Laucks, M.L., 2001. An evaluation of the community aerosol inlet for the NCAR C-130 research aircraft. Journal of Atmospheric and Oceanic Technology 18, 1387–1397.

Bower, K.N., et al., 2000. ACE-2 HILLCLOUD. An overview of the ACE-2 ground-based cloud experiment. Tellus 52B, 750–778.

Brenguier, J.L., et al., 2000. An overview of the ACE-2 CLOUDYCOLUMN closure experiment. Tellus 52B, 815–827.

Celik, F., Marwitz, J.D., 1999. Droplet spectra broadening by ripening process: Part I. Roles of curvature and salinity of cloud droplets. Journal of Atmospheric Science 56, 3091–3105.

Charlson, R.J., Lovelock, J.E., Andreae, M.O., Warren, S.G., 1987. Oceanic phytoplankton, atmospheric sulfur, cloud albedo and climate. Nature 326, 655–661.

Clarke, A.D., Varner, J.L., Eisele, F., Mauldin, R.L., Tanner, D., Litchy, M., 1998. Particle production in the remote marine atmosphere: cloud outflow and subsidence during ACE-1. Journal of Geophysical Research 103, 16397–16409.

Dibb, J.E., Talbot, R.W., Scheuer, E.M., Blake, D.R., Blake, N.J., Gregory, G.L., Sachse, G.W., Thornton, D.C., 1999. Aerosol chemical composition and distribution during the Pacific Exploratory Mission (PEM) Tropics. Journal of Geophysical Research 104, 5785–5800.

Frank, E.R., Lodge, J.P., 1967. Morphological identification of air-borne particles with electron microscope. Journal of Microscopy 6, 449–456.

Fuzzi, S., et al., 1994. Multiphase chemistry and acidity of clouds at Kleiner Feldberg. Journal of Atmospheric Chemistry 19, 87–106.

Galloway, J.N., Zhao, D., Thomson, V.E., Chang, L.H., 1996. Nitrogen mobilization in the United States of America and the People's Republic of China. Atmospheric Environment 30, 1551–1561.

Garrett, T.J., Hobbs, P.V., 1995. Long-range transport of continental aerosols over the Atlantic Ocean and their effects on cloud structures. Journal of Atmospheric Science 52, 2977–2984.

Gieray, R., et al., 1997. Phase partitioning of aerosol constituents in cloud base on single-particles and bulk analysis. Atmospheric Environment 31, 2491–2502.

Gurciullo, C., Lerner, B., Sievering, H., Pandis, S.N., 1999. Heterogeneous sulfate production in the remote marine environment: cloud processing and sea-salt particle contributions. Journal of Geophysical Research 104, 21719–21731.

Hallberg, A., Ogren, J.A., Noone, K.J., Okada, K., Heintzenberg, J., Svenningsson, I.B., 1994. The influence of aerosol particle composition on cloud droplet formation. Journal of Atmospheric Chemistry 19, 153–171.

Hegg, D.A., Hobbs, P.V., 1986. Sulfate and nitrate chemistry in cumuliform clouds. Atmospheric Environment 20, 901–909.

Hegg, D.A., Radke, L.F., Hobbs, P.V., 1990. Particle production associated with marine clouds. Journal of Geophysical Research 96, 18727–18733.

Hoppel, W.A., Fitzgerald, J.W., Frick, G.M., Larson, R.E., Mack, E.J., 1990. Aerosol size distributions and optical properties found in the marine boundary layer over the Atlantic Ocean. Journal of Geophysical Research 95, 3659–3686.

Hudson, J.G., Da, X., 1996. Volatility and size of cloud condensation nuclei. Journal of Geophysical Research 101, 4435–4442.

Hudson, J.G., Li, H., 1995. Microphysical contrasts in Atlantic stratus. Journal of Atmospheric Science 52, 3031–3040.

Hudson, J.G., Rogers, C.F., 1986. Relationship between critical supersaturation and cloud droplet size: implications for cloud mixing processes. Journal of Atmospheric Science 3, 2341–2359.

Hudson, J.G., Xie, Y., 1999. Vertical distributions of cloud condensation nuclei spectra over the summertime northeast Pacific and Atlantic Oceans. Journal of Geophysical Research 104, 30219–30229.

Ishizaka, Y., Kurahashi, Y., Tsuruta, H., 1995. Microphysical properties of winter stratiform clouds over the Southwest Islands Area in Japan. Journal of the meteorological Society of Japan 73, 1137–1151.

Kagawa, M., Ishizaka, Y., Ohta, K., 2001. Concentrations of ions and selenium in cloud water and aerosols. Report for 2000 Special Research Project of the Institute of Hydrospheric–Atmospheric Sciences of Nagoya University: Activities of Clouds in the Transformation of Continental Pollutants in Marine Atmosphere. IHAS, Nagoya, Japan, pp. 51–56 (in Japanese).

Kaneyasu, N., Hobbs, P.V., Ishizaka, Y., Qian, G.W., 2001. Aerosol properties around marine tropical cumulus clouds. Journal of Geophysical Research 106, 14435–14445.

Kato, N., Akimoto, H., 1992. Anthropogenic emissions of SO_2 and NO_x in Asia: emission inventories. Atmospheric Environment 26A, 2997–3017.

Kramer, M., Beltz, N., Schell, D., Schutz, L., Sprengard-Eichel, C., Wurzler, S., 2000. Cloud processing of continental aerosol particles: experimental investigations for different drop size. Journal of Geophysical Research 105, 11739–11752.

Laj, P., et al., 1997a. Cloud processing of soluble gases. Atmospheric Environment 31, 2589–2598.
Laj, P., et al., 1997b. Experimental evidence for in-cloud production of aerosol sulphate. Atmospheric Environment 31, 2503–2514.
Martin, L.R., Damschen, D.E., 1981. Aqueous oxidation of sulfur dioxide by hydrogen peroxide at low pH. Atmospheric Environment 15, 1621–1651.
Martinsson, B.G., Swietlicki, E., Hansson, H.C., Wiedensohler, A., Noone, K.J., Ogren, J.A., Hallberg, A., 1992. Elemental composition of fog interstitial particle size fractions and hydrophobic fractions related to fog droplet nucleation scavenging. Tellus 44B, 593–603.
Matsumoto, K., Takana, H., 1996. Formation and dissociation of atmospheric particulate nitrate and chloride: an approach based on phase equilibrium. Atmospheric Environment 30, 639–648.
McInnes, L., Covert, D., Baker, B., 1997. The number of sea-salt, sulfate, and carbonaceous particles in the marine atmosphere: EM measurements consistent with the ambient size distribution. Tellus 49B, 300–313.
Muyshondt, A., Anand, N.K., McFarland, A.R., 1996. Turbulent deposition of aerosol particles in large transport tubes. Aerosol Science and Technology 24, 107–116.
Noone, K.J., et al., 1992. Changes in aerosol size- and phase distributions due to physical and chemical processes in fog. Tellus 44B, 489–504.
Noonkester, V.R., 1984. Droplet spectra observed in marine stratus cloud layers. Journal of Atmospheric Science 41, 829–845.
Parungo, F., Nagamoto, C., Zhou, M., Hansen, A.D.A., Harris, J., 1994. Aeolian transport of aerosol black carbon from China to the ocean. Atmospheric Environment 28, 3251–3260.
Perry, K.D., Hobbs, P.V., 1994. Further evidence for particle nucleation in clear air adjacent to marine cumulus clouds. Journal of Geophysical Research 99, 22803–22818.
Prospero, J.M., Savoie, D.L., 1989. Effect of continental sources on nitrate concentrations over the Pacific Ocean. Nature 339, 687–689.
Pui, D.Y.H., Romay-Novas, F., Liu, B.Y.H., 1987. Experimental study of particles deposition in bends of circular cross section. Aerosol Science and Technology 7, 301–315.
Savoie, D.L., Prospero, J.M., 1989. Comparison of oceanic and continental sources of on-sea-salt sulphate over the Pacific Ocean. Nature 339, 685–687.
Schwarzenbock, A., Wieprecht, W., Mertes, S., Heintzenberg, J., 2001. Cloud droplet residual sizes and residual mass concentrations in specific drop size classes. Journal of Aerosol Science 32, s205–s206.
Shantz, N.C., Leaitch, W.R., Caffrey, P.F., 2003. Effect of organics of low solubility on the growth rate of cloud droplets. Journal of Geophysical Research 108 (D5), 4168. doi:10.1029/2002JD002540.
Stelson, A.W., Seinfeld, J.H., 1982. Thermodynamic prediction of the water activity, NH_4NO_3 dissociation constant, density and refractive index for the NH_4NO_3–$(NH_4)_2SO_4$–H_2O system at 25 °C. Atmospheric Environment 16, 2507–2514.
Stephens, G.L., Platt, C.M.R., 1987. Aircraft observations of the radiative and microphysical properties of stratocumulus and cumulus cloud fields. Journal of Atmospheric Science 38, 235–247.
Streets, D.G., et al., 2003. An inventory of gaseous and primary aerosol emission in Asia in the year 2000. Journal of Geophysical Research 108 (D21), 8809. doi:10.1029/2002JD003093.
Suzuki, K., Horibe, T., 2001. Developments of an aircraft-borne centrifugal collector of cloud water and aerosol samplers. Report for 2000 Special Research Project of the Institute of Hydrospheric–Atmospheric Sciences of Nagoya University: Activities of Clouds in the Transformation of Continental Pollutants in Marine Atmosphere. IHAS, Nagoya, Japan, pp. 12–16 (in Japanese).
Svenningsson, B., et al., 1997. Cloud droplet nucleation scavenging in relation to the size and hydroscopic behaviour of aerosol particles. Atmospheric Environment 31, 2463–2475.
Thornton, D.C., Bandy, A.R., Blomquist, B.W., Driedger, A.R., Wade, T.P., 1999. Sulfur dioxide distribution over the Pacific Ocean 1991–1996. Journal of Geophysical Research 104, 5845–5854.
Twomey, S., Warner, J., 1967. Comparison of measurements of cloud droplets and cloud nuclei. Journal of Atmospheric Science 24, 702–703.
Watanabe, K., Ishizaka, Y., Takenaka, C., 2001. Chemical characteristics of cloud water over the Japan Sea and the Northwestern Pacific Ocean near the central part of Japan: airborne measurements. Atmospheric Environment 35, 645–655.

Zhang, D., Iwasaka, Y., 2001. Chlorine deposition on dust particles in marine atmosphere. Geophysical Research Letters 28, 3613–3616.

Zhang, D., Shi, G., Iwasaka, Y., Hu, M., 2000. Mixture of sulfate and nitrate in coastal atmospheric aerosols: individual particle studies in Qingdao (36°04′N, 120°21′E). Atmospheric Environment 34, 2669–2679.

Zhang, D., Shi, G., Iwasaka, Y., 2001. Soot particles and their impacts on the mass cycle in Tibetan atmosphere. Atmospheric Environment 35, 5883–5894.